

# Chaos in high-dimensional dynamical systems

Iaroslav Ispolatov,<sup>1,\*</sup> Michael Doebeli,<sup>2,†</sup> and Vaibhav Madhok<sup>2,‡</sup>

<sup>1</sup>*Departamento de Fisica, Universidad de Santiago de Chile, Santiago, Chile*

<sup>2</sup>*Department of Zoology and Department of Mathematics,  
University of British Columbia, Vancouver, BC V6T 1Z4 Canada*

For generally dissipative dynamical systems we study what fraction of solutions exhibit chaotic behavior depending on the dimensionality  $d$  of the phase space. We find that a system of  $d$  globally coupled ODE with quadratic, cubic, and fourth-order non-linearities with random coefficients and initial conditions, the probability of a trajectory to be chaotic increases universally from  $\sim 10^{-5} - 10^{-4}$  for  $d = 3$  to essentially one for high  $d$ . In the limit of large  $d$ , the invariant measure of the dynamical systems exhibits universal scaling that depends on the degree of non-linearity but does not depend on the choice of coefficients, and the largest Lyapunov exponent converges to a universal scaling limit. Using statistical arguments, we provide analytical explanations for the observed scaling and for the probability of chaos.

In many standard texts, a transition from classical concepts to statistical mechanics is justified by the prevalence of chaotic and ergodic behavior as more degrees of freedom are considered. However, quantitative details of such transitions from integrability to chaos apparently remain elusive. In this paper we consider the fundamental question of the likelihood of chaos in general dissipative dynamical systems in continuous time as a function of the dimension of phase space. We note that existing results about the probability of chaos vs. dimensions in discrete maps [? ?] as well as in a Hamiltonian system of locally-coupled oscillators [?] cannot be applied to dissipative dynamical systems in continuous time with an arbitrary degree of non-linearity and global coupling. In the following we show that the probability that the solution of a generic  $d$ -dimensional system of ODEs with quadratic, cubic or fourth-order non-linearities (1,2,3) is chaotic universally increases from  $\sim 10^{-4} - 10^{-5}$  for  $d = 3$  to essentially 1 for large  $d$ . The results of our numerical investigations are then explained analytically, using a combination of scaling and statistical methods. These results are an extension and generalization of an investigation of the prevalence of chaos in the dynamics of high-dimensional phenotypes under frequency-dependent natural selection [?]. However, the applicability and significance of our results is not limited to biological evolution, and in principle extends to dynamical systems in statistical and nonlinear physics, hydrodynamics, plasma physics, control theory, and social and economic studies.

To investigate the statistics of trajectories, we numerically solve the following systems of equations

$$\frac{dx_i}{dt} = \sum_{j=1}^d b_{ij}x_j + \sum_{j,k=1}^d a_{ijk}x_jx_k - x_i^3, \quad i = 1, \dots, d, \quad (1)$$

$$\begin{aligned} \frac{dx_i}{dt} &= \sum_{j=1}^d b_{ij}x_j + \sum_{j,k=1}^d a_{ijk}x_jx_k + \\ &+ \sum_{j,k,l=1}^d c_{ijkl}x_jx_kx_l - x_i^5, \quad i = 1, \dots, d, \end{aligned} \quad (2)$$

$$\begin{aligned} \frac{dx_i}{dt} &= \sum_{j=1}^d b_{ij}x_j + \sum_{j,k=1}^d a_{ijk}x_jx_k + \\ &+ \sum_{j,k,l=1}^d c_{ijkl}x_jx_kx_l - x_i^3|x_i|, \quad i = 1, \dots, d. \end{aligned} \quad (3)$$

The coefficients  $\{a\}$ ,  $\{b\}$ , and  $\{c\}$  were randomly and independently drawn from Gaussian distributions with zero mean and unit variance. The last highest-order terms,  $-x_i^3$ ,  $-x_i^5$ , and  $-x_i^3|x_i|$  were introduced to ensure confinement of all trajectories to a finite volume of phase space, thus excluding divergent scenarios. In [?], we integrated system (1) for each dimension  $d$  using a 4th-order Runge-Kutta method for 50 sets of the coefficients  $b_{ij}$  and  $a_{ijk}$ , each with 4 sets of random initial conditions. This procedure was repeated for the current work. For (2) and (3), the numerical simulations are significantly more complex and computationally extensive. We therefore integrated systems (2) and (3) for 50 sets of the coefficients  $b_{ij}$ ,  $a_{ijk}$  and  $c_{ijkl}$  each with a single set of random initial conditions. For each trajectory we determined the Largest Lyapunov Exponent (LLE) by perturbing the trajectory by a small magnitude  $\delta x_0$  in a random direction, integrating both trajectories in parallel for time  $\tau$ , measuring the distance between trajectories  $\delta x_\tau$ , rescaling the separation between trajectories back to  $\delta x_0$ , and continuing this for the course of the simulation. The LLE was calculated as

$$\lambda = \frac{1}{\tau} \ln \left( \frac{\|\delta x_\tau\|}{\|\delta x_0\|} \right), \quad (4)$$

and subsequently averaged over the trajectory. The time of integration was chosen such that the average LLE saturated to a constant value. In cases when a trajectory converged to a stable fixed point and the LLE was persistently negative, the integration was stopped. By visually inspecting many trajectories we concluded that trajectories with average Largest Lyapunov Exponent (LLE)  $\lambda \geq 0.1$  can be considered chaotic, while trajectories with  $\lambda \leq -0.1$  are converging to stable fixed points. We refer to the remaining trajectories with  $|\lambda| \leq 0.1$  as “quasiperiodic”.

Our main result is that for all considered types of non-linearity the probability of chaos increases with the dimension

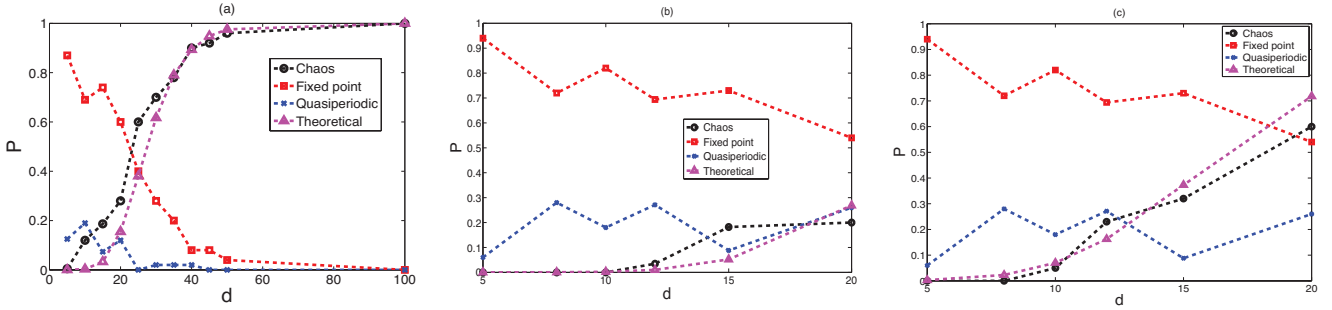


FIG. 1: Probability of different types of dynamics as a function of dimension  $d$  of the phenotypic space. The numerically measured probability of occurrence of chaos (black line) and our theoretical estimate (magenta line; see text). (a) For each dimension  $d$ , the system (1) was integrated using a 4th-order Runge-Kutta method for 50 sets of the coefficients  $b_{ij}$ ,  $a_{ijk}$ ,  $c_{ijkl}$  each with 4 sets of random initial conditions. The probabilities are estimated by computing the for Largest Lyapunov Exponent (LLE) as described in the main text. The results are in agreement with [? ]. (b) For each dimension  $d$ , the system (2) was integrated using a 4th-order Runge-Kutta method for 50 sets of the coefficients  $b_{ij}$ ,  $a_{ijk}$ ,  $c_{ijkl}$  for a single set of random initial conditions. The probabilities are estimated by computing the for Largest Lyapunov Exponent (LLE) as described in the main text. (c) For each dimension  $d$ , the system (3) was integrated using a 4th-order Runge-Kutta method for 50 sets of the coefficients  $b_{ij}$ ,  $a_{ijk}$ ,  $c_{ijkl}$  for a single set of random initial conditions. The probabilities are obtained by computing the for Largest Lyapunov Exponent (LLE) as described in the main text.

of the phase space. In particular, the numerical simulations for (1) as well as the theoretical predictions (see below) for (2,3) suggest that, essentially all trajectories become chaotic for  $d \sim 100$ . Our simulations also indicate that already for intermediate dimensions  $d \gtrsim 15$ , the majority of chaotic trajectories essentially fill out the available phase space, i.e., become ergodic (Fig. 2). In such a regime the probability density  $P(x_i)$  for each coordinate of the chaotic attractor approaches a universal scaling form that depends neither on the choice of coefficients  $\{a\}$ ,  $\{b\}$ ,  $\{c\}$  nor on the dimension  $d$ , Fig. 3.

Below we explain the scaling and statistical properties of the large- $d$  limit of (1,2,3), using the system (1) as an example. In the supplementary material, we extend our arguments to explain our results for (2) and (3). First, consider the scaling of the spatial coordinates,  $x_i \sim d^\alpha$ , illustrated in Fig. 2(a). Since the coefficients  $b_{ij}$  and  $a_{ijk}$  in (1) are drawn randomly, it is reasonable to assume that each coordinate has a similar scale,  $x_i \sim x$  and (1) becomes

$$\frac{dx}{dt} \sim x \sum_{j=1}^d b_{ij} + x^2 \sum_{j,k=1}^d a_{ijk} - x^3. \quad (5)$$

Here the  $b_{ij}$  and  $a_{ijk}$  are identically distributed random terms with zero mean and unit variance, and a typical value of the sum of  $N$  such terms is the standard deviation  $\sqrt{N}$ , which yields the following scaling relation:

$$\frac{dx}{dt} \sim \sqrt{dx} + dx^2 - x^3. \quad (6)$$

Introducing new variables,

$$\begin{aligned} y &= \frac{x}{d} \\ \theta &= td^2, \end{aligned} \quad (7)$$

we convert (6) into

$$\frac{dy}{d\theta} \sim \frac{y}{d^{3/2}} + y^2 - y^3 \quad (8)$$

with two universal,  $d$ -independent terms and a linear term that vanishes in the limit of large  $d \gg 1$ . The transformation (7) explains the observed scaling of the size of chaotic attractors,  $x = yd$  (Fig. 2, 3), and of the largest Lyapunov exponent, whose dimension is the inverse of time,  $1/t = d^2/\theta$  (Fig. 4). The transformation also shows that the linear term  $\sum_{j=1}^d b_{ij}x_j$  in (1) as well as quadratic terms in (2,3) do not affect the dynamics for large  $d$ . In the general case of a dynamical system similar to (1,2,3) with the  $n$ th-order highest nonlinear term and the  $|x_i|^m sign(x_i)$ ,  $m > n$  diagonal confining term,

$$\frac{dx_i}{dt} = \sum_{j_1, \dots, j_n=1}^d g_{i,j_1, \dots, j_n} x_{j_1} \dots x_{j_n} - |x_i|^m sign(x_i), \quad (9)$$

the same analysis yields

$$\begin{aligned} y &= \frac{x}{d^\alpha}, \quad \alpha = \frac{n}{2(m-n)} \\ \theta &= td^\beta, \quad \beta = \frac{n(m-1)}{2(m-n)} \end{aligned} \quad (10)$$

To explain the shape of the universal probability density  $P(y)$  shown in Fig. 3, we ignore the irrelevant low-order terms and replace the leading nonlinear term (quadratic in (1)) by a stochastic function  $f(\theta)$ . This is done observing that for large  $d$ , the majority of the terms comprising the  $\sum_{j,k=1}^d a_{ijk}x_jx_k$  do not contain  $x_i$  and could be approximated as independent

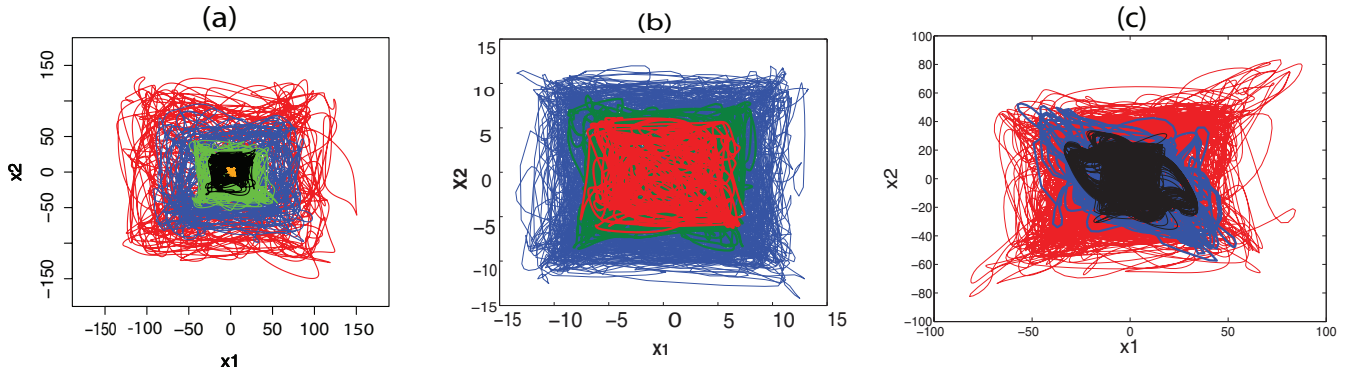


FIG. 2: Color online. (a) Examples of projections of ergodic chaotic trajectories for dynamics described by (1) for  $d = 15$  (yellow),  $d = 30$  (black),  $d = 50$  (green),  $d = 100$  (blue) and  $d = 150$  (red). The figure is analogous to Figure S2 in [?] and illustrates the scaling  $x_i \sim d$ . (b) Examples of projections of ergodic chaotic trajectories for the dynamics described by (2) for  $d = 15$  (red),  $d = 20$  (green),  $d = 30$  (blue). The figure illustrates the scaling  $x_i \sim d^{3/4}$ . (c) Examples of projections of ergodic chaotic trajectories for dynamics described by (3) for  $d = 12$  (black),  $d = 15$  (blue),  $d = 20$  (red), The figure illustrates the scaling  $x_i \sim d^{3/2}$ .

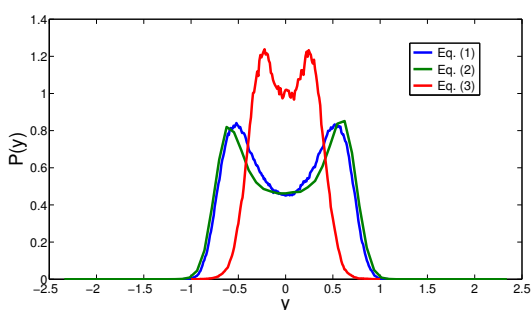


FIG. 3: Examples of the density distributions (invariant measure) of the scaled variable(s) averaged over time. (a) Dynamical system (1) - probability density distribution for  $d = 150$  for an arbitrary phase space coordinate that is rescaled as  $y = x/d$ . (b) Dynamical system (2) - probability density distribution for  $d = 30$  for an arbitrary phase space coordinate that is rescaled as  $y = x/d^{3/4}$  (c) Dynamics system (3) - probability density distribution for  $d = 20$  for an arbitrary phase space coordinate that is rescaled  $y = x/d^{3/2}$ . Once the system is in the ergodic regime, the distribution is universal and independent of the dimension  $d$  of phenotype space, of the particular choice of coefficients or of the phase space coordinate.

random variables. Since  $\langle a^2 \rangle = 1$  by definition, it follows from the Central Limit theorem that such sum is a Gaussian random variable with the dispersion  $d^2 \langle x^2 \rangle^2$ . Thus  $f(t)$  is a Gaussian random process with this dispersion and the correlation time of the order of  $\lambda$ . We approximate  $f(t)$  by a jump process which takes constant Gaussian-distributed values  $f_i$  during time intervals drawn from a uniform distribution with

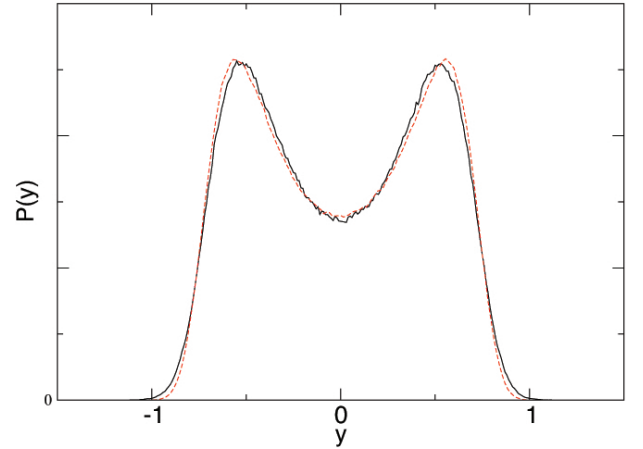


FIG. 4: The probability density for the scaled coordinate  $P(y)$  vs.  $y$  for  $d = 150$  (solid black line) and the histogram of the solution of (20) (dashed red line)

an average period  $\tau$ . We solve to the resulting, scaling equation

$$\frac{dy}{d\theta} = f(\theta) - y^3 \quad (11)$$

self-consistently, computing  $\langle y^2 \rangle^2$  from the histogram of the trajectory  $y(\theta)$ . Varying  $\tau$ , we find the best fit to the observed  $P(x/d)$  which is shown in Fig. 5. Given the evidently approximate nature of the temporal behaviour of  $f(\theta)$  the fit seems quite satisfactory and yields  $\tau^* = 3.85$  which is fairly close to the large- $d$  asymptotics of inverse LLE,  $1/\lambda_{infty} \approx 4.26$ . Now we provide a statistical explanation for the growth of probability of chaos with the dimension  $d$  such as shown in

Fig. 1. Consider stationary points of the dynamical system (1). Since a system of  $d$  third-order algebraic equations generally has  $3d$  solutions (sometime coinciding), the dynamical system (1) has  $3d$  stationary points  $x^*$ . The system is chaotic or quasiperiodic if all these stationary points are unstable in at least one direction, i.e., if at each stationary point  $x^*$  at least one eigenvalue of the local Jacobian matrix  $J(x^*)$  has a positive real part. We assume that for sufficiently high  $d$ , all Jacobian eigenvalues are statistically independent. This assumption of weakening correlations between dimensions as the number of dimensions increase is a rather strong approximation without which it seems impossible to derive analytical estimates, and which seems to result in reasonable results (see below). Then, denoting the probability that the real part of an eigenvalue is negative by  $P_{neg}$ , the probability that at least one out of  $d$  eigenvalues of the Jacobian at a stationary point has a positive real part is  $1 - P_{neg}^d$ . Hence the probability of chaos is

$$P_{chaos} = (1 - P_{neg}^d)^{3d}, \quad (12)$$

indicating that for any  $P_{neg} = 1 - \epsilon < 1$ , for the dimension  $d > 1/\epsilon$  the system is predominantly chaotic. Specifically, if  $x^*$  is a stationary point of (1), the elements of the Jacobian matrix  $J(x^*) = \{J_{ij}(x^*)\}_{i,j=1}^d$  consist of two terms,

$$\begin{aligned} J_{ij}(x^*) &= \sum_{k=1}^d (a_{ijk} + a_{ikj})x_k^* - 3x_i^{*2}\delta_{ij} \\ &= J_{ij}^{(1)} + J_{ij}^{(2)}, \end{aligned} \quad (13)$$

where  $\{\delta_{ij}\}$  is the identity matrix. Here we ignored the irrelevant for large  $d$  linear term  $\sum_{j=1}^d b_{ij}x_j$ . We assume that the distribution of  $x_i^*$  is the same as for the coordinates  $x_i$  themselves and is given by the universal invariant measure shown in Figs. 3 and 5. We also consider the two terms  $J_{ij}^{(1)}$  and  $J_{ij}^{(2)}$  as statistically independent. The first term,  $J_{ij}^{(1)} = \sum_{k=1}^d (a_{ijk} + a_{ikj})x_k^*$ , is a sum of  $d \gg 1$  of random variables with zero mean and a finite variance. Taking into account that the dispersions of  $a_{ijk}$  are one, and  $x_i$  and  $\{a_{ijk}\}$  are uncorrelated (this follows from the observed independence of  $P(x)$  of the choice of  $\{a\}$ ) the Central Limit theorem states that this sum is a Gaussian-distributed variable with zero mean and variance  $\sigma^2 = 2d\langle x^2 \rangle$ . It follows from the “Girko’s circular law” [?] that eigenvalues of a random  $d \times d$ -matrix with Gaussian-distributed elements with zero mean and unit variance are uniformly distributed on a disk in the complex plane with radius  $\sqrt{d}$ . Thus, the eigenvalues of  $J_{ij}^{(1)}$  are uniformly distributed on a disk with radius  $d\sqrt{2\langle x^2 \rangle}$ . The probability for an eigenvalue of  $J_{ij}^{(1)}$  to have real part  $rd\sqrt{2\langle x^2 \rangle}$ , with  $|r| \leq 1$ , is then proportional to the length of the chord intersecting the radius of the disk at the point  $r$ ,

$$P_c(r) = \frac{2\sqrt{1-r^2}}{\pi}. \quad (14)$$

(The factor  $2/\pi$  normalizes  $P_c(r)$  to one.) The probability distribution of the second, diagonal, term of the Jacobian,  $J_{ij}^{(2)} = -3x_i^{*2}\delta_{ij}$  is defined by the universal scaling form  $P(x/d)$ , given by (20) and shown in Figs. 3,5. Both  $J_{ij}^{(1)}$  and  $J_{ij}^{(2)}$  contribute terms of order  $d^2$  to the eigenvalues of the Jacobian. The contribution from  $J_{ij}^{(1)}$  may have a positive or a negative real part with equal probability  $1/2$ . The contribution from  $J_{ij}^{(2)}$  is always negative and has magnitude  $3y^2$  with probability  $P(y)$ . Thus the probability that the sum of the two contributions has negative real part is

$$P_{neg} = \frac{1}{2} + \int_{-\infty}^{+\infty} P(y)dy \int_0^{3y^2/\beta} P_c(r)dr. \quad (15)$$

where  $\chi \equiv \sigma/d^2 = \sqrt{2\langle y^2 \rangle}$ . Here the  $1/2$  term reflects the probability that the eigenvalue of  $J_{ij}^{(1)}$  has a negative real part and the magnitude of  $J_{ij}^{(2)}$  does not matter, while the double integral gives the probability that the positive real part of  $J_{ij}^{(1)}$  is smaller than the contribution  $-3y^2$  from  $J_{ij}^{(2)}$ . Integration on  $dr$  produces

$$\begin{aligned} P_n &= \frac{1}{2} \left[ 1 + \int_{|y|>\sqrt{\beta/3}} P(y)dy \right] \\ &+ \int_{|y|<\sqrt{\beta/3}} \frac{\sin^{-1}(3y^2/\beta) + 3y^2/\beta\sqrt{1-(3y^2/\beta)^2}}{\pi} P(y)dy. \end{aligned} \quad (16)$$

Using the numerical data for  $P(y)$  shown in Fig. 3,5, we calculate  $\chi \approx 0.675$  and perform numerical integration of  $P(y)$  to obtain  $P_{neg} \approx 0.85$ . Substituting this value into Eq. (16) above provides a reasonable fit for the observed probability of chaos, as illustrated in Fig. 6

To summarize, we have presented numerical evidence that the behaviour of generic dynamical systems becomes completely chaotic as the dimension of the phase space exceeds  $\sim 100$ . We provide simple analytic explanations to the observed ubiquity of chaos and universality of the density distribution of chaotic trajectories. One of the goals of this work was to illustrate the transition to chaos and ergodicity in high-dimensional phase space, a frequently pronounced yet rarely justified maxima in the formal justification of statistical mechanics. Ironically, in explaining our results, we had to use the scaling and probabilistic arguments borrowed from the statistical physics.

---

\* Electronic address: [jaros007@gmail.com](mailto:jaros007@gmail.com)

† Electronic address: [doebeli@zoology.ubc.ca](mailto:doebeli@zoology.ubc.ca)

‡ Electronic address: [vmadhok@gmail.com](mailto:vmadhok@gmail.com)

## SUPPLEMENTARY MATERIAL

### LYAPUNOV EXPONENTS

We can derive an analytical expression for the measure of chaos, as quantified by the Lyapunov exponents, as a function of the system dimension. We use the arguments provided above for the fact that the eigenvalues of  $J^1$  are uniformly distributed over the circular disk in the complex plane. Given the distribution  $P_c(r)$  of real parts of rescaled eigenvalues of  $J^1$ , the distribution of the largest real part of the rescaled eigenvalue is given by

$$P_{max}(\lambda) = P_c(\lambda)d \left[ \int_{-1}^{\lambda} P_c(r)dr \right]^{d-1}. \quad (17)$$

Here,  $P_c(\lambda)$  is the probability that the largest eigenvalue is equal to  $\lambda$ , and the integral term gives the probability that the remaining eigenvalues are less than  $\lambda$ . The multiplicative factor  $d$  comes in due to the fact that any of the eigenvalues could be the largest.

$$\langle \lambda \rangle = \int \lambda P_{max}(\lambda) d\lambda \quad (18)$$

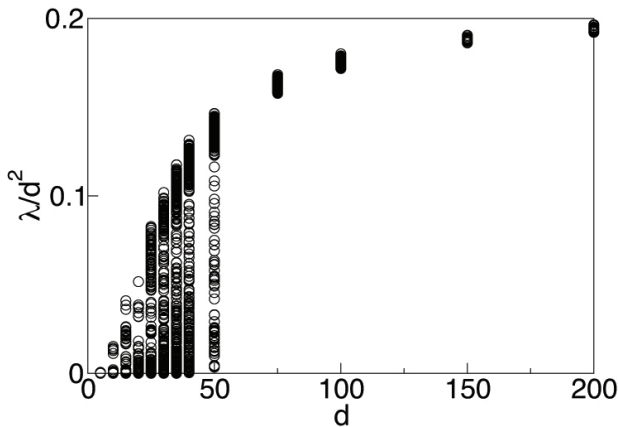


FIG. 5: The scaled LLE  $\lambda/d^2$  as a function of the dimension  $d$  of phase space for (1). For large  $d$ ,  $\lambda \rightarrow \lambda^* \approx 0.235$ .

Using Eq. ?? to evaluate Eq. 17 and integrating Eq. 18 we obtain

$$\langle \lambda \rangle = \lambda^* - \int \left[ \frac{\sin^{-1}(x) + \pi/2 + x\sqrt{1-x^2}}{\pi} \right]^d dx, \quad (19)$$

where  $\lambda^*$  is a constant determining the upper value of the largest rescaled eigenvalue. Equations 17, 18 and 19 are valid

for the rescaled eigenvalues for systems with  $m$ th order nonlinearities. That is, the expression 19 captures the behavior of  $\lambda = \frac{\lambda_m}{d^m}$ , the rescaled eigenvalue of the Jacobian of the matrix associated with a system having  $m$ th order nonlinearities. In fig ??

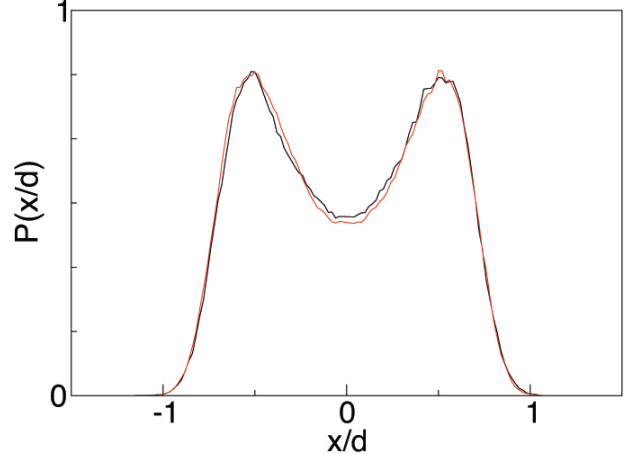


FIG. 6: The probability density for the scaled coordinate  $P(y)$  vs.  $y$  for  $d = 150$  (solid black line) and the histogram of the solution of (20) (dashed red line)

### THE PROBABILITY DENSITY

To explain the shape of the universal probability density  $P(y)$  shown in Fig. 3, we ignore the irrelevant low-order terms and replace the leading nonlinear term (quadratic in (1)) by a stochastic function  $f(\theta)$ . This is done observing that for large  $d$ , the majority of the terms comprising the  $\sum_{j,k=1}^d a_{ijk}x_jx_k$  do not contain  $x_i$  and could be approximated as independent random variables. Since  $\langle a^2 \rangle = 1$  by definition, it follows from the Central Limit theorem that such sum is a Gaussian random variable with the dispersion  $d^2\langle x^2 \rangle^2$ . Thus  $f(t)$  is a Gaussian random process with this dispersion and the correlation time of the order of  $\lambda$ . We approximate  $f(t)$  by a jump process which takes constant Gaussian-distributed values  $f_i$  during time intervals drawn from a uniform distribution with an average period  $\tau$ . We solve to the resulting, scaling equation

$$\frac{dy}{d\theta} = f(\theta) - y^3 \quad (20)$$

self-consistently, computing  $\langle y^2 \rangle^2$  from the histogram of the trajectory  $y(\theta)$ . Varying  $\tau$ , we find the best fit to the observed  $P(x/d)$  which is shown in Fig. 8.